Antiferromagnetic superconductors with effective-mass anisotropy in magnetic fields

Yuuichi Suginishi and Hiroshi Shimahara

Department of Quantum Matter Science, ADSM, Hiroshima University, Higashi-Hiroshima 739-8530, Japan
(Received 3 March 2006; published 24 July 2006)

We derive critical field H_{c2} equations for antiferromagnetic s-wave, $d_{x^2-y^2}$-wave, and d_{xy}-wave superconductors with effective-mass anisotropy in three dimensions, where we take into account (i) the Jaccarino-Peter mechanism of magnetic-field-induced superconductivity (FISC) at high fields, (ii) an extended Jaccarino-Peter mechanism that reduces the Pauli paramagnetic pair-breaking effect at low fields where superconductivity and an antiferromagnetic long-range order with a canted spin structure coexist, and (iii) the Fulde-Ferrell-Larkin-Ovchinnikov (FFLO or LOFF) state. As an example, experimental phase diagrams observed in organic superconductor κ-$(BETS)_2FeBr_4$ are theoretically reproduced. In particular, the upper critical field of low-field superconductivity is well reproduced without any additional fitting parameter other than those determined from the critical field curves of the FISC at high fields. Therefore, the extended Jaccarino-Peter mechanism seems to occur actually in the present compound. It is predicted that the FFLO state does not occur in the FISC at high fields in contrast to the compound λ-$(BETS)_2FeCl_4$, but it may occur in low-field superconductivity for s-wave and $d_{x^2-y^2}$-wave pairings. We also briefly discuss a possibility of compounds that exhibit unconventional behaviors of upper critical fields.

I. INTRODUCTION

Recently, magnetic-field-induced superconductivity (FISC) has been observed in organic superconductors λ-$(BETS)_2FeCl_4$ and κ-$(BETS)_2FeBr_4$,[1–3] where BETS is bis-(ethylenedithio)tetraselenafulvalene. In these salts, localized spins on Fe^{3+} exhibit antiferromagnetic long-range order at ambient pressure at low temperatures. The FISC in these compounds is considered to be due to the Jaccarino-Peter mechanism,[4,5] where the localized spins are aligned uniformly at high fields. Konoike *et al.* have observed in the compound κ-$(BETS)_2FeBr_4$ that superconductivity coexists with the antiferromagnetic long-range order in a low-field region around the zero field.[3] They have fitted the experimental phase diagrams by Fisher's theory[6] based on the Jaccarino-Peter mechanism. The resultant upper critical field of low-field superconductivity is much smaller than their experimental data. They have suggested that the reason for the discrepancy is that the Jaccarino-Peter-Fisher theory does not take into account the antiferromagnetic long-range order at low fields.[3]

In recent works, one of the authors has extended the Jaccarino-Peter mechanism to antiferromagnetic superconductors with canted spin structures in magnetic fields.[7,8] The canted spin structure generates the ferromagnetic moments that create exchange fields acting on the conduction electrons through Kondo interactions. If the Kondo interactions are antiferromagnetic, the exchange fields partly cancel the Zeeman energy. As a result, the Pauli paramagnetic pair-breaking effect can be largely reduced, and the upper critical field can exceed the Pauli paramagnetic limit (Chandrasekhar and Clongston limit).[9] This mechanism occurs even in the presence of the orbital pair-breaking effect.[8] We call this mechanism an extended Jaccarino-Peter mechanism in this paper. Since the canted antiferromagnetic phase occurs in the compound κ-$(BETS)_2FeBr_4$ for $\mathbf{H} \| c$,[3,10] we apply the mechanism to this compound.

In the compound κ-$(BETS)_2FeBr_4$, the FISC has been observed both for $\mathbf{H} \| c$ and $\mathbf{H} \| a$.[3] The phase diagrams for $\mathbf{H} \| c$ and $\mathbf{H} \| a$ are rather different, and it is attributed to the anisotropy of the Fermi surface and the Kondo interactions between the localized spins and the conduction electrons. We take into account the Fermi surface anisotropy by effective masses.

The effective-mass model was introduced in Ginzburg-Landau equations by Ginzburg.[11,12] Hohenberg and Werthamer[13] pointed out that detailed structures of the Fermi surface affect the upper critical field. Rieck and Scharnberg[14] and Langmann[15] obtained general equations for arbitrary Fermi surfaces. Xu *et al.*[16] and Kim *et al.*[17] calculated the upper critical fields of mixed d-wave and s-wave superconductors with effective-mass anisotropy. Recently, Kita and Arai[18] have formulated an equation for the upper critical field, taking into account the Fermi surface anisotropy and the gap anisotropy on the basis of the Rieck and Scharnberg theory.[14] They have performed the quantitative calculations of the upper critical fields for type-II superconductors Nb, $NbSe_2$, and MgB_2 using Fermi surfaces obtained by first-principles calculations.[18]

A theory of the upper critical field for layered superconductors has been proposed by Lebed and Yamaji,[19] and developed by Lebed and Hayashi.[20] They have found that when the layer spacing is large, the upper critical field exhibits a reentrant transition or an enhancement at low temperatures in the quantum region, due to an effect of dimensional crossover induced by the magnetic field.[19] In the compounds κ-$(BETS)_2FeBr_4$, however, since the upper critical field of the low-field superconductivity did not exhibit either a reentrant transition or an enhancement in the experimental phase diagrams, the dimensional crossover does not seem to take place. Therefore, from a phenomenological consideration, we use the effective-mass model as an approximation instead of strict equations in Refs. 19 and 20. The effective-mass model is adequate in the Ginzburg-Landau region for layered superconductors.

In this paper, first, we derive critical field equations for s-wave, $d_{x^2-y^2}$-wave, and d_{xy}-wave superconductors with effective-mass anisotropy in three directions, taking into account both orbital and paramagnetic pair-breaking effects. Secondly, we take into account the extended Jaccarino-Peter mechanism. Lastly, we reproduce the phase diagrams of κ-(BETS)$_2$FeBr$_4$ including both the FISC and low-field superconductivity.

We also examine the possibility of the FFLO state. The FFLO state has extensively been studied[21] since pioneering works by Fulde and Ferrell, and Larkin and Ovchinnikov.[22] The state is taken into account by an extension of the BCS mean-field theory to include the possibility of finite center-of-mass momenta $\mathbf{q}$'s. In this study, we adopt a model in which $\mathbf{q} \parallel \mathbf{H}$ is assumed following Gruenberg and Gunther,[23] since we consider the situation in which substantial orbital pair-breaking effect is present. In the organic compounds λ-(BETS)$_2$FeCl$_4$, the possibility of the FFLO state in the FISC has been pointed out by Uji *et al.*[1] and Balicas *et al.*,[2] and also examined theoretically.[24,25] The shape of the phase boundary of the FISC is well reproduced by taking into account the FFLO state.[25] Tanatar *et al.* have also argued that the FFLO state may occur in λ-(BETS)$_2$GaCl$_4$ from their experimental data.[26] Recently, the quasi-two-dimensional heavy-fermion superconductor CeCoIn$_5$ has been believed to exhibit the FFLO state.[27–31] Adachi and Ikeda[32] and Won *et al.*[33] have calculated the critical fields for $d_{x^2-y^2}$-wave pairing taking into account the FFLO state in connection with CeCoIn$_5$.

This paper is constructed as follows. In the next section, we extend the theory of the critical field to the systems with anisotropic Fermi surfaces. The s-wave, $d_{x^2-y^2}$-wave, and d_{xy}-wave pairing superconductors are examined. In Sec. III, we take into account the extended Jaccarino-Peter mechanism.[7,8] In Sec. IV, we apply the present theory to the organic superconductor κ-(BETS)$_2$FeBr$_4$. We compare experimental and theoretical phase diagrams. The final section is devoted to the summary and a discussion.

II. UPPER CRITICAL FIELD IN SYSTEMS WITH EFFECTIVE-MASS ANISOTROPY

In this section, we derive critical field equations for s-wave, $d_{x^2-y^2}$-wave, and d_{xy}-wave superconductors with an effective-mass anisotropy. We consider the electron system with the energy dispersion

$$\epsilon(\mathbf{p}) = \frac{p_x^2}{2m_x} + \frac{p_y^2}{2m_y} + \frac{p_z^2}{2m_z} = \sum_{\nu=1}^{3} \frac{p_\nu^2}{2m_\nu} \tag{1}$$

and the pairing interaction

$$\mathcal{H}' = \int d^3\mathbf{r} \int d^3\mathbf{r}' \psi_\uparrow^\dagger(\mathbf{r})\psi_\uparrow(\mathbf{r})V(\mathbf{r}-\mathbf{r}')\psi_\downarrow^\dagger(\mathbf{r}')\psi_\downarrow(\mathbf{r}'), \tag{2}$$

where we have defined $\mathbf{p}=(p_1,p_2,p_3)=(p_x,p_y,p_z)$ and introduced anisotropic effective masses $m_x=m_1$, $m_y=m_2$, and $m_z=m_3$. In the magnetic field $\mathbf{H}=\mathbf{B}=\mathrm{rot}\mathbf{A}$, the Hamiltonian is written as

$$\mathcal{H} = \mathcal{H}_0 + \mathcal{H}_m + \mathcal{H}', \tag{3}$$

where

$$\mathcal{H}_0 = \sum_\sigma \int d^3\mathbf{r}\psi_\sigma^\dagger(\mathbf{r}) \sum_{\nu=1,2,3} \frac{1}{2m_\nu}\left[-i\hbar\frac{\partial}{\partial x_\nu} - \frac{e}{c}A_\nu(\mathbf{r})\right]^2 \psi_\sigma(\mathbf{r}),$$

$$\mathcal{H}_m = -\int d^3\mathbf{r}\mu_e\mathbf{H}\cdot\left[\sum_{\sigma\sigma'}\psi_\sigma^\dagger(\mathbf{r})\boldsymbol{\sigma}_{\sigma\sigma'}\psi_{\sigma'}(\mathbf{r})\right]. \tag{4}$$

Here, $\psi_\sigma(\mathbf{r})$ denotes the field operator which annihilates an electron of spin σ at a point $\mathbf{r}\equiv(x,y,z)\equiv(x_1,x_2,x_3)$. We have defined the electronic magnetic moment $\mu_e=-g_e\mu_B/2$ with the Bohr magneton $\mu_B=\hbar|e|/(2mc)$ and the g factor of the conduction electrons g_e. We use the units such that $c=k_B=\hbar=1$ unless it is explicitly expressed.

We define the S^z axis in the spin space along the direction of $\mathbf{H}$. We should note that the S^z axis does not necessarily coincide with the z axis of the electron coordinate depending on the direction of the $\mathbf{H}$. Therefore, we have

$$\mathcal{H}_m = -\sum_\sigma \int d^3\mathbf{r}\,\sigma h\psi_\sigma^\dagger(\mathbf{r})\psi_\sigma(\mathbf{r}), \tag{5}$$

where $h\equiv\mu_e H$ with $H=|\mathbf{H}|$, and $\sigma=+1$ and -1 for up and down spin states, respectively.

We apply the BCS mean-field approximation to the interaction Hamiltonian (2) as

$$\mathcal{H}' = -\int d^3\mathbf{r}\int d^3\mathbf{r}'\left[\Delta_\downarrow(\mathbf{r},\mathbf{r}')\psi_\uparrow^\dagger(\mathbf{r})\psi_\downarrow^\dagger(\mathbf{r}')\right.$$
$$\left. + \Delta_\downarrow^*(\mathbf{r},\mathbf{r}')\psi_\downarrow(\mathbf{r}')\psi_\uparrow(\mathbf{r})\right], \tag{6}$$

defining the order parameter

$$\Delta_{-\sigma}(\mathbf{r},\mathbf{r}') \equiv -V(\mathbf{r}-\mathbf{r}')\langle\psi_{-\sigma}(\mathbf{r}')\psi_\sigma(\mathbf{r})\rangle. \tag{7}$$

We define the center-of-mass coordinate $\mathbf{R}=(\mathbf{r}+\mathbf{r}')/2$ and the relative coordinate $\boldsymbol{\rho}=\mathbf{r}-\mathbf{r}'$, and redefine the gap function as $\Delta_{-\sigma}(\mathbf{R},\boldsymbol{\rho})$. By following the procedure of Refs. 34 and 35, we obtain the linearized gap equation

$$\Delta_{-\sigma}(\mathbf{r},\mathbf{p}) = -T\sum_n \int \frac{d^3\mathbf{p}'}{(2\pi)^3}\int d^3\boldsymbol{\rho}\exp(i\mathbf{p}'\cdot\boldsymbol{\rho})V(\mathbf{p}-\mathbf{p}')$$
$$\times G_\sigma^{(0)}(-\mathbf{p}',-i\omega_n)\int\frac{d^3\mathbf{p}''}{(2\pi)^3}$$
$$\times \exp(i\mathbf{p}''\cdot\boldsymbol{\rho})\,G_{-\sigma}^{(0)}(\mathbf{p}'',-i\omega_n)$$
$$\times \exp(i\boldsymbol{\rho}\cdot\boldsymbol{\Pi})\Delta_{-\sigma}(\mathbf{r},\mathbf{p}') \tag{8}$$

near the second-order phase-transition point. We could examine both orbital and paramagnetic pair-breaking effects with Eq. (8). In the derivation of Eq. (8), it is assumed that the spatial variation of vector potential $\mathbf{A}$ is sufficiently slow. Therefore, the order parameter becomes a slowly varying function of the center-of-mass coordinate. We have defined

$$\mathbf{\Pi} = - i \hbar \nabla - \frac{2e}{c} \mathbf{A}(\mathbf{r}), \qquad (9)$$

the Matsubara frequencies $\omega_n = (2n+1)\pi T$ with integer $n = 0, \pm 1, \pm 2, \ldots$, and the free-electron Green's function

$$G_\sigma^{(0)}(\mathbf{p}, i\omega_n) = \frac{1}{i\omega_n - \epsilon(\mathbf{p}) + \sigma h + \mu}. \qquad (10)$$

We introduce $\widetilde{\mathbf{p}} = (\widetilde{p}_x, \widetilde{p}_y, \widetilde{p}_z) = (\widetilde{p}_1, \widetilde{p}_2, \widetilde{p}_3)$ with $\widetilde{p}_\nu = (\widetilde{m}/m_\nu)^{1/2} p_\nu$, so that the dispersion relation becomes isotropic as

$$\epsilon(\mathbf{p}) = \widetilde{\epsilon}(\widetilde{\mathbf{p}}) \equiv \frac{\widetilde{p}^2}{2\widetilde{m}} = \frac{1}{2\widetilde{m}}(\widetilde{p}_x^2 + \widetilde{p}_y^2 + \widetilde{p}_z^2) \qquad (11)$$

in the $\widetilde{\mathbf{p}}$ space, where $\widetilde{m} \equiv (m_x m_y m_z)^{1/3}$. We also introduce $\widetilde{\mathbf{r}} = (\widetilde{x}_1, \widetilde{x}_2, \widetilde{x}_3) = (\widetilde{x}, \widetilde{y}, \widetilde{z})$ with $\widetilde{x}_\nu = (m_\nu/\widetilde{m})^{1/2} x_\nu$ and $\partial/\partial \widetilde{x}_\nu = (\widetilde{m}/m_\nu)^{1/2} \partial/\partial x_\nu$, so that $\mathbf{p} \cdot \mathbf{r} = \widetilde{\mathbf{p}} \cdot \widetilde{\mathbf{r}}$. We also define the operator $\widetilde{\mathbf{\Pi}}$ with

$$\widetilde{\boldsymbol{\rho}} \cdot \widetilde{\mathbf{\Pi}} \equiv \boldsymbol{\rho} \cdot \mathbf{\Pi}, \qquad (12)$$

where $\boldsymbol{\rho} = (\rho_1, \rho_2, \rho_3)$ and $\widetilde{\rho}_\nu = (m_\nu/\widetilde{m})^{1/2} \rho_\nu$. We will calculate the explicit form of $\widetilde{\mathbf{\Pi}}$ afterward.

We replace $|\widetilde{\mathbf{p}}|$ and $|\widetilde{\mathbf{p}}'|$ in $V(\mathbf{p} - \mathbf{p}')$, $\Delta_{-\sigma}(\mathbf{r}, \mathbf{p})$, and $\Delta_{-\sigma}(\mathbf{r}, \mathbf{p}')$ with the Fermi momentum $\widetilde{p}_F$ since electrons with momenta $\widetilde{\mathbf{p}}$ and $\widetilde{\mathbf{p}}'$ near the Fermi surface mainly contribute to the gap equation. Therefore, we write $V(\mathbf{p} - \mathbf{p}')$ and $\Delta_{-\sigma}(\mathbf{r}, \mathbf{p})$ as $V(\hat{\mathbf{p}}, \hat{\mathbf{p}}')$ and $\Delta_{-\sigma}(\widetilde{\mathbf{r}}, \hat{\widetilde{\mathbf{p}}})$, respectively, with unit vectors $\hat{\mathbf{p}} = \mathbf{p}/|\mathbf{p}|$ and $\hat{\widetilde{\mathbf{p}}} = \widetilde{\mathbf{p}}/|\widetilde{\mathbf{p}}|$.

After simple algebra using Eq. (10), we obtain

$$\Delta_{-\sigma}(\widetilde{\mathbf{r}}, \hat{\widetilde{\mathbf{p}}}) = -\pi T \sum_{|\omega_n| < \omega_D} \widetilde{N}(0) \int \frac{d\Omega_{\hat{\widetilde{\mathbf{p}}}'}}{4\pi} V(\hat{\mathbf{p}}, \hat{\mathbf{p}}')$$
$$\times \int_0^\infty dt e^{-[|\omega_n| - i\sigma h \, \mathrm{sgn}(\omega_n)]t}$$
$$\times \exp\left[\frac{t}{2i} \mathrm{sgn}(\omega_n) \widetilde{\mathbf{v}}_F(\hat{\widetilde{\mathbf{p}}}') \cdot \widetilde{\mathbf{\Pi}} \right] \Delta_{-\sigma}(\widetilde{\mathbf{r}}, \hat{\widetilde{\mathbf{p}}}'), \qquad (13)$$

where we have defined $\widetilde{\mathbf{v}}_F(\widetilde{\mathbf{p}}) \equiv \widetilde{\mathbf{p}}/\widetilde{m}$ and the density of states at the Fermi energy $N(0) \equiv \widetilde{m} \widetilde{p}_F/(2\pi^2\hbar^2)$.[35] Since Eq. (13) does not depend on the spin value σ, we omit the spin suffix from now on. By redefining $\widetilde{\mathbf{p}}' = t\widetilde{\mathbf{v}}_F(\hat{\widetilde{\mathbf{p}}}')/2 = t\widetilde{v}_F\hat{\widetilde{\mathbf{p}}}'/2$ and summing up the Matsubara frequencies, the gap equation (13) acquires the form

$$\Delta(\widetilde{\mathbf{r}}, \hat{\widetilde{\mathbf{p}}}) = -\frac{TN(0)}{2\widetilde{v}_F} \int d^3\widetilde{\mathbf{p}}' V(\hat{\mathbf{p}}, \hat{\mathbf{p}}') \frac{1 - e^{-2\widetilde{p}'\omega_D/\widetilde{v}_F}}{\widetilde{p}'^2 \sinh(2\pi T\widetilde{p}'/\widetilde{v}_F)}$$
$$\times \cos\left[\frac{2\widetilde{p}'}{\widetilde{v}_F} h + \widetilde{\mathbf{p}}' \cdot \widetilde{\mathbf{\Pi}} \right] \Delta(\widetilde{\mathbf{r}}, \hat{\widetilde{\mathbf{p}}}'). \qquad (14)$$

It is obvious that if we rewrite the integral variable $\widetilde{\mathbf{p}}$ as $\mathbf{p}$, the linearized gap equation (14) is similar to those obtained by many authors.[12–14,34–38] The differences between Eq. (14) and the equations obtained so far for isotropic systems are

that the vector potential $\mathbf{A}$ is scaled as $\widetilde{A}_\nu = (m_\nu/\widetilde{m})^{1/2} A_\nu$ in $\widetilde{\mathbf{\Pi}}$, and that the pairing interaction $V(\hat{\mathbf{p}}, \hat{\mathbf{p}}')$ is deformed in the $\widetilde{\mathbf{p}}$-space anisotropic superconductivity. The former scale transformation in $\mathbf{A}$ has been studied in Ginzburg-Landau theory[11,12,39] for s-wave pairing. For s-wave pairing, since $V(\hat{\mathbf{p}}, \hat{\mathbf{p}}') = V(\hat{\widetilde{\mathbf{p}}}, \hat{\widetilde{\mathbf{p}}}')$, Eq. (14) is exactly reduced to the equations for the system with the isotropic Fermi surface, except the scale of A_ν, which results in the scaling $\widetilde{H}_\nu = (m_\nu/\widetilde{m})^{1/2} H_\nu$. Therefore, the only difference due to the Fermi-surface anisotropy is that the critical field in the ν direction is enhanced or reduced by the factor $(\widetilde{m}/m_\nu)^{1/2}$. The latter deformation of $V(\hat{\mathbf{p}}, \hat{\mathbf{p}}')$ occurs because $V(\hat{\mathbf{p}}, \hat{\mathbf{p}}') \neq V(\hat{\widetilde{\mathbf{p}}}, \hat{\widetilde{\mathbf{p}}}')$ for anisotropic superconductivity. We take into account the deformation of the pairing interaction in the $\widetilde{\mathbf{p}}$ space. These changes affect the mass anisotropy dependence of the critical field.

Now, we derive a more explicit form of the upper critical field equation. We take the z axis in the direction where the effective mass is the largest. The compounds with layered structures with large layer spacing are approximately described by the models with $m_z \gg m_x, m_y$. For example, in the application to the organic superconductor κ-$(BETS)_2FeBr_4$, we take the x and y axes along c and a axes of the compounds, respectively. We study a quasi-two-dimensional superconductor under magnetic fields parallel to the layers ($\mathbf{H} \| x$ or $\mathbf{H} \| y$) hereafter. We derive the critical field equations only for $\mathbf{H} \| x$, because those for $\mathbf{H} \| y$ are obtained by exchanging m_x and m_y.

We assume the uniform magnetic field $\mathbf{H}$ in the $-x$ direction parallel to the layers, which is expressed by a vector potential $\mathbf{A} = (0, 0, -Hy)$. Then, we obtain the explicit form of $\widetilde{\mathbf{\Pi}}$ as

$$\widetilde{\mathbf{\Pi}} = \left(-i\hbar \frac{\partial}{\partial \widetilde{x}}, \; -i\hbar \frac{\partial}{\partial \widetilde{y}}, \; -i\hbar \frac{\partial}{\partial \widetilde{z}} - \frac{2|e|}{c} \frac{\widetilde{m}}{\sqrt{m_y m_z}} H\widetilde{y} \right)$$

from Eqs. (9) and (12). We define the differential operators

$$\eta_{\widetilde{\mathbf{r}}} = \frac{1}{\sqrt{2\kappa_x}} (\widetilde{\Pi}_y - i\widetilde{\Pi}_z),$$

$$\eta_{\widetilde{\mathbf{r}}}^\dagger = \frac{1}{\sqrt{2\kappa_x}} (\widetilde{\Pi}_y + i\widetilde{\Pi}_z), \qquad (15)$$

which satisfy the bosonic commutation relations, where

$$\kappa_x \equiv \frac{\widetilde{m}}{\sqrt{m_y m_z}} \frac{2|e|H}{c}. \qquad (16)$$

The factor $\widetilde{m}/\sqrt{m_y m_z}$ is due to the effective-mass anisotropy.

We consider pairing interactions of the form

$$V(\hat{\mathbf{p}}, \hat{\mathbf{p}}') = -g_\alpha \gamma_\alpha(\hat{\mathbf{p}}) \gamma_\alpha(\hat{\mathbf{p}}'), \qquad (17)$$

where $\gamma_\alpha(\hat{\mathbf{p}})$ denotes the symmetry function of symmetry α and $\alpha = s$, $d_{x^2-y^2}$, d_{xy}, and so on. The symmetry function $\gamma_\alpha(\hat{\mathbf{p}})$ is normalized so that $\langle [\gamma_\alpha(\hat{\mathbf{p}})]^2 \rangle = 1$, where the average on the Fermi surface $\langle \cdots \rangle$ is defined by $\langle \cdots \rangle = \int d\Omega_{\mathbf{p}} \rho(0, \theta, \varphi) \times (\cdots) / \int d\Omega_{\mathbf{p}} \rho(0, \theta, \varphi)$, where $\rho(0, \theta, \varphi)$ denotes the angle-

dependent density of states on the Fermi surface. The gap function is proportional to the symmetry function $\gamma_\alpha(\hat{\mathbf{p}})$ and expanded by the Abrikosov functions $\phi_n(\tilde{\mathbf{r}})$ of the Landau-level indexes $n = 0, 1, 2, \ldots$ as

$$\Delta(\tilde{\mathbf{r}}, \hat{\tilde{\mathbf{p}}}) = \sum_{n=0}^{\infty} \Delta_n^\alpha \gamma_\alpha(\hat{\mathbf{p}}) \phi_n(\tilde{\mathbf{r}}) e^{i\tilde{q}\tilde{x}}. \tag{18}$$

The Abrikosov functions $\phi_n(\tilde{\mathbf{r}})$ are expressed as

$$\phi_n(\tilde{\mathbf{r}}) = \frac{1}{\sqrt{n!}} (\eta_{\tilde{\mathbf{r}}}^\dagger)^n \phi_0(\tilde{\mathbf{r}}), \tag{19}$$

where $\phi_0(\tilde{\mathbf{r}})$ denotes the solution of $\eta_{\tilde{\mathbf{r}}} \phi_0(\tilde{\mathbf{r}}) = 0$. In the gap function (18), we have taken into account the possibility of nonzero $\tilde{q}$ for the FFLO state, where $\tilde{q} \equiv (\tilde{m}/m_x)^{1/2} |\mathbf{q}|$. The linearized gap equation (14) can be written as

$$\Delta_n^\alpha = N(0) g_\alpha \sum_{n'} E_{nn'}^\alpha \Delta_{n'}^\alpha \tag{20}$$

with

$$E_{nn'}^\alpha = \delta_{nn'} E_0^\alpha - D_{nn'}^\alpha, \tag{21}$$

where we have defined

$$E_0^\alpha = \frac{T}{2\tilde{v}_F} \int d^3\tilde{\mathbf{p}} [\gamma_\alpha(\hat{\mathbf{p}})]^2 \frac{1 - e^{2\tilde{p}\omega_D/\tilde{v}_F}}{\tilde{p}^2 \sinh(2\pi T\tilde{p}/\tilde{v}_F)},$$

$$D_{nn'}^\alpha = -\frac{T}{2\tilde{v}_F} \int d^3\tilde{\mathbf{p}} [\gamma_\alpha(\hat{\mathbf{p}})]^2 \frac{1 - e^{2\tilde{p}\omega_D/\tilde{v}_F}}{\tilde{p}^2 \sinh(2\pi T\tilde{p}/\tilde{v}_F)} e^{i(n'-n)\tilde{\varphi}}$$

$$\times \left[\sum_{j=1}^{\infty} d_{nn'}^{(j)}(\tilde{p}, \tilde{\theta})(\delta_{n'-n,2j} + \delta_{n'-n,-2j}) + d_{nn'}^{(0)}(\tilde{p}, \tilde{\theta}) \delta_{nn'} \right] \tag{22}$$

and

$$d_{nn'}^{(j)}(\tilde{p}, \tilde{\theta}) \equiv \exp\left[-\frac{\kappa_x}{4} \tilde{p}^2 \sin^2 \tilde{\theta} \right] \sum_{k=0}^{\min(n,n')} \left[-\frac{\kappa_x}{2} \tilde{p}^2 \sin^2 \tilde{\theta} \right]^{k+j}$$

$$\times \frac{\sqrt{n!\, n'!}}{k!\,(k+2j)!\,[\min(n,n')-k]!}$$

$$\times \cos\left[\frac{2\tilde{p}}{\tilde{v}_F} \left(h + \frac{\tilde{q}\tilde{v}_F}{2} \cos \tilde{\theta} \right) \right] - \delta_{nn'} \delta_{j,0}. \tag{23}$$

More explicit expressions of the matrix elements $D_{nn'}^s$, $D_{nn'}^{d_{x^2-y^2}}$, and $D_{nn'}^{d_{xy}}$ are given below. Defining the zero-field transition temperature $T_c^{(0)}$, the linearized gap equation (20) is written as

$$\log \frac{T}{T_c^{(0)}} \Delta_n^\alpha = -\sum_{n'=0}^{\infty} D_{nn'}^\alpha \Delta_{n'}^\alpha. \tag{24}$$

The transition temperature and the critical field are given by the condition that Eq. (20) has a nontrivial solution of Δ_n^α for the first time when the magnetic field and temperature decrease, respectively, where $\tilde{q}$ is optimized.

A. The case of *s*-wave pairing

For *s*-wave pairing, we insert $\gamma_s(\hat{\mathbf{p}}) = 1$ into Eq. (21). It is easily verified by integrating over $\tilde{\varphi}$ that $E_{nn'}^s = 0$ for $n \neq n'$. Therefore, the matrix elements $D_{nn'}^s$ in the linearized gap equation (24) are expressed as

$$D_{nn'}^s = -\frac{\pi T}{\tilde{v}_F} \int_0^\infty d\tilde{p} \int_0^\pi \sin \tilde{\theta} d\tilde{\theta} \frac{d_{nn'}^{(0)}(\tilde{p}, \tilde{\theta}) \delta_{nn'}}{\sinh(2\pi T\tilde{p}/\tilde{v}_F)}. \tag{25}$$

B. The case of $d_{x^2-y^2}$-wave pairing

We consider $d_{x^2-y^2}$-wave pairing interaction given by Eq. (17) with $\gamma_{d_{x^2-y^2}}(\hat{\mathbf{p}}) = C_1(\hat{p}_x^2 - \hat{p}_y^2)$, where $(\hat{p}_x, \hat{p}_y) = (p_x, p_y)/\sqrt{p_x^2 + p_y^2}$. The function $\gamma_{d_{x^2-y^2}}(\hat{\mathbf{p}})$ is rewritten as

$$\gamma_{d_{x^2-y^2}}(\hat{\mathbf{p}}) = C_1 \frac{m_x \tilde{p}_x^2 - m_y \tilde{p}_y^2}{m_x \tilde{p}_x^2 + m_y \tilde{p}_y^2} = C_1 \left[\frac{2m_x}{m_x + m_y \tan^2 \tilde{\theta} \cos^2 \tilde{\varphi}} - 1 \right], \tag{26}$$

where we have defined the polar coordinates $(\tilde{\theta}, \tilde{\varphi})$ taking the $\tilde{p}_x$ axis as the polar axis, so that $\tilde{\theta}$ is measured from the $\tilde{p}_x$ axis, and $\tilde{\varphi}$ is measured from the $\tilde{p}_y$ axis. Therefore, in the linearized gap equation (24), the matrix elements $D_{nn'}^{d_{x^2-y^2}}$ are written as

$$D_{nn'}^{d_{x^2-y^2}} = D_{nn'}^{d_{x^2-y^2}(0)} \delta_{nn'} + \sum_{j=1}^{\infty} D_{nn'}^{d_{x^2-y^2}(j)} (\delta_{n,n'+2j} + \delta_{n+2j,n'}), \tag{27}$$

where $D_{nn'}^{d_{x^2-y^2}(j)}$ is defined by

$$D_{nn'}^{d_{x^2-y^2}(j)} = -\frac{\pi T}{\tilde{v}_F} \int_0^\infty d\tilde{p} \int_0^\pi \sin \tilde{\theta} d\tilde{\theta} \frac{C_{d_{x^2-y^2}}^{(j)}(\tilde{\theta}) d_{nn'}^{(j)}(\tilde{p}, \tilde{\theta})}{\sinh(2\pi T\tilde{p}/\tilde{v}_F)}, \tag{28}$$

with

$$C_{d_{x^2-y^2}}^{(j)}(\tilde{\theta}) = \left[1 + \frac{2\sqrt{m_x m_y}}{m_x + m_y} \right] \left[\frac{c(\tilde{\theta}) - 1}{c(\tilde{\theta}) + 1} \right]^j \left\{ \delta_{j,0} - 2c(\tilde{\theta}) + 4j[c(\tilde{\theta})]^2 + 2[c(\tilde{\theta})]^3 \right\}, \tag{29}$$

and $c(\tilde{\theta}) \equiv 1/\sqrt{1 + (m_y/m_x)\tan^2 \tilde{\theta}}$. The matrix equation (24) is decoupled two sets of equations for $\Delta_n^{d_{x^2-y^2}}$ of even and odd n's.

C. The case of d_{xy}-wave pairing

Next, we consider d_{xy}-wave pairing interaction with

$$\gamma_{d_{xy}}(\hat{\mathbf{p}}) = C_2 \hat{p}_x \hat{p}_y = C_2 \frac{\sqrt{m_x m_y} \tan \tilde{\theta} \cos \tilde{\varphi}}{m_x + m_y \tan^2 \tilde{\theta} \cos^2 \tilde{\varphi}}. \tag{30}$$

The matrix elements $D_{nn'}^{d_{xy}}$ take the form

$$D_{nn'}^{d_{xy}} = D_{nn'}^{d_{xy}(0)} \delta_{nn'} + \sum_{j=1}^{\infty} D_{nn'}^{d_{xy}(j)} (\delta_{n,n'+2j} + \delta_{n+2j,n'}), \quad (31)$$

where $D_{nn'}^{d_{xy}(j)}$ is defined by

$$D_{nn'}^{d_{xy}(j)} = -\frac{\pi T}{\tilde{v}_F} \int_0^{\infty} d\tilde{p} \int_0^{\pi} \sin\tilde{\theta}\, d\tilde{\theta} \frac{C_{d_{xy}}^{(j)}(\tilde{\theta}) d_{nn'}^{(j)}(\tilde{p},\tilde{\theta})}{\sinh(2\pi T\tilde{p}/\tilde{v}_F)}, \quad (32)$$

with

$$C_{d_{xy}}^{(j)}(\tilde{\theta}) = \left[1 + \frac{m_x + m_y}{2\sqrt{m_x m_y}}\right] \left\{ 2c(\tilde{\theta})\{1 - [c(\tilde{\theta})]^2\}\delta_{j,0} \right.$$
$$\left. - \frac{4j}{[c(\tilde{\theta})]^{2j-1}}\left[\frac{c(\tilde{\theta}) - 1}{c(\tilde{\theta}) + 1}\right]^j \right\}. \quad (33)$$

The order parameter components $\Delta_0^{d_{xy}}$ and $\Delta_1^{d_{xy}}$ couple only with $\Delta_{2n}^{d_{xy}}$ and $\Delta_{2n+1}^{d_{xy}}$, respectively, where $n = 1, 2, \dots$. Therefore the matrix equation (24) for d_{xy}-wave pairing is decoupled into two sets of equations for $\Delta_n^{d_{xy}}$ of even and odd n's.

III. EXTENDED JACCARINO-PETER MECHANISM

In this section, we review an extended Jaccarino-Peter mechanism in antiferromagnetic superconductors.[7,8] We have formulated the upper critical field equation of the conduction electron system in the previous section. Now, we shall introduce a localized spin system that is coupled with the conduction electron system through the Kondo interaction J_K. We consider a situation in which the antiferromagnetic long-range order has canted spin structures in magnetic fields. Then, ferromagnetic moments are induced in the localized spins and create exchange fields on the conduction electrons. The exchange fields partly or completely cancel the magnetic fields in the Zeeman energy terms of the conduction electrons when $J_K > 0$. The exchange fields are not real magnetic fields in the sense that they only modify the Zeeman energy terms but not the vector potential. On the other hand, the ferromagnetic moments also create real internal magnetic fields. However, such internal magnetic fields are weak when the localized spins are spatially separated from the conduction electrons. Therefore, we neglect them in this study.

We examine the case in which the antiferromagnetic transition occurs at a temperature much higher than the superconducting transition temperature and thus the magnetic ordered state is rigid. Therefore, we neglect modification of the magnetic structure by occurrence of superconductivity. Strictly speaking, the localized spin state is modified by the mobile electrons, and the state of the total system should be determined self-consistently.[40] However, we consider a model in which such modification has already been included and the canted spin structure occurs as a result.

We modify the extended Jaccarino-Peter mechanism[7,8] for the system with anisotropic Kondo interactions, introducing Kondo coupling constants J_K^μ between the localized spins and the conduction electrons of the x_μ component in spin space. When the magnetic field is oriented to the $-x_\mu$ direction, where $\mu = 1, 2, 3$, we replace $\mathcal{H}_m$ in Eq. (4) with the effective Hamiltonian

$$\tilde{\mathcal{H}}_m = -\sum_\sigma \int d^3\mathbf{r}\, \sigma\tilde{h}_\mu \psi_\sigma^\dagger(\mathbf{r})\psi_\sigma(\mathbf{r}), \quad (34)$$

where $\tilde{h}_\mu$ denotes the effective Zeeman energy. Therefore, in the critical field equations derived in the previous section, the Zeeman energy h is replaced with $\tilde{h}_\mu$. For $H \leq H_{AF}$, $\tilde{h}_\mu$ is given by

$$\tilde{h}_\mu = \left(1 - \frac{g_s z_K J_K^\mu}{g_e z J}\right) h = \left(1 - \frac{J_K^\mu}{J'_{AF}}\right) h \quad (35)$$

with $J'_{AF} \equiv g_e z J/(g_s z_K)$. In Eq. (35), z, z_K, J, and g_s denote number of antiferromagnetic bonds for a given site, number of lattice sites that participate in the Kondo interaction with the conduction electrons at $\mathbf{r}$, coupling constant of the exchange interaction of the localized spins, and the g factor of the localized spins, respectively. Here, H_{AF} denotes the critical field of the antiferromagnetic phase, which is given by $H_{AF} = 2zJ\bar{S}/g_s\mu_B$, where $\bar{S}$ denotes the magnitude of the localized spins. Therefore, when $0 < J_K^\mu < 2J'_{AF}$, the Pauli paramagnetic pair-breaking effect is reduced in antiferromagnetic superconductors.

For $H \geq H_{AF}$, since the spins are aligned uniformly, the effective Zeeman energy $\tilde{h}_\mu$ is given by

$$\tilde{h}_\mu = h - z_K J_K^\mu \bar{S}. \quad (36)$$

Because the second term is a negative constant when $J_K^\mu > 0$, the present mechanism is reduced to the conventional Jaccarino-Peter mechanism. The Zeeman energy is completely compensated at $H = z_K J_K^\mu \bar{S}/|\mu_e| \equiv H_{cent}^\mu$. It is noted that FISC occurs only when $H_{cent}^\mu/H_{AF} = J_K^\mu/J'_{AF} \gtrsim 1$.[7,8]

IV. APPLICATION TO AN ORGANIC SUPERCONDUCTOR

In this section, we apply the present theory to the antiferromagnetic organic superconductor κ-$(BETS)_2FeBr_4$ taking the x and y axes along the crystallographic c and a axes, respectively. Therefore, we write the effective masses as $m_x = m_c$, $m_y = m_a$, and $m_z = m_b$, and the anisotropic Kondo interactions as $J_K^1 = J_K^c$ and $J_K^2 = J_K^a$. In κ-$(BETS)_2FeBr_4$, the canted spin structure was observed when $\mathbf{H} \| c$, and we can apply the extended Jaccarino-Peter theory. However, for the magnetic field parallel to the magnetic easy axis, i.e., $\mathbf{H} \| a$, the canted spin structure have not been observed and the details of the metamagnetic transition have not been revealed. Therefore, we do not apply the present theory to the low-field region for $\mathbf{H} \| a$.

It is convenient to introduce a constant

$$a_m \equiv \left(\frac{\tilde{m}}{m_b}\right)^{1/4}\left(\frac{\tilde{v}_F}{2\pi T_c^{(0)}}\right)^2 \frac{2|e|}{c}, \quad (37)$$

with which κ_x and κ_y are expressed as

$$\kappa_x = a_m H\left(\frac{m_c}{m_a}\right)^{1/4}\left[\frac{2\pi T_c^{(0)}}{\tilde{v}_F}\right]^2,$$
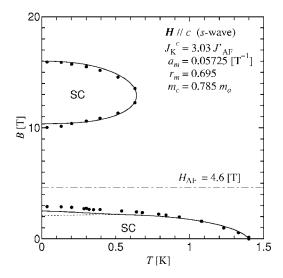
FIG. 1. Theoretical phase diagram for *s*-wave pairing in the magnetic fields parallel to the *c* axis. Here, SC stands for superconductivity. The solid and dotted curves show boundaries of superconductivity in the presence and the absence of the FFLO state, respectively. The closed circles show the experimental data of the superconducting transition points for **H**∥*c* in κ-(BETS)$_2$FeBr$_4$ by Konoike *et al.* (Ref. 3). The dot-dashed line shows the critical field of the antiferromagnetic phase.

$$\kappa_y = a_m H \left(\frac{m_a}{m_c}\right)^{1/4} \left[\frac{2\pi T_c^{(0)}}{\bar{v}_F}\right]^2. \tag{38}$$

We also define the strength ratio of the paramagnetic and orbital pair-breaking effects

$$r_m \equiv \frac{h/2\pi T_c^{(0)}}{a_m H}. \tag{39}$$

We explain the procedure to analyze the experimental phase diagram with the present theory. Our critical field equations contain five microscopic parameters: a_m, m_c/m_a, r_m, J_K^c, and J_K^a. First, we fit the experimental data of the critical field of the FISC for **H**∥*c* with the parameters a_m, m_c/m_a, r_m, and J_K^c. Secondly, using the parameter values of a_m, m_c/m_a, and r_m determined in the first step, we fit the data of the FISC for **H**∥*a* with a single parameter J_K^a. It is noted that all five parameters are determined only from the curves of the FISC for **H**∥*c* and **H**∥*a*. Crudely speaking, the curve of the FISC can be characterized by three real numbers, that is, the magnetic field where the transition temperature is maximum, the maximum transition temperature, and the width of the magnetic fields at $T=0$. Therefore, we obtain six real numbers from the two experimental data of the FISC, which sufficiently determine all five microscopic parameters. Lastly, using those five parameters determined in the first and second steps, we calculate the upper critical field of low-field superconductivity for **H**∥*c*, where the canted spin structure coexists. In this last step, we do not use any additional fitting parameter.

We carry out this procedure for *s*-wave, $d_{x^2-y^2}$-wave, and d_{xy}-wave pairings. In Figs. 1–7, we set $T_c^{(0)}=1.4$ K and $H_{AF}=4.6$ T, which have been observed in the compounds
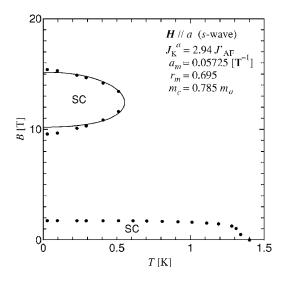
FIG. 2. Theoretical phase diagram for *s*-wave pairing in the magnetic fields parallel to the *a* axis. The notations are the same as those in Fig. 1. Since the canted spin structure does not occur for **H**∥*a* at low field, the upper critical field of low-field superconductivity has not been calculated.

κ-(BETS)$_2$FeBr$_4$. For all pairing symmetries examined, the theoretical curves agree well with the experimental data, as shown in Figs. 1–6. In particular, the agreements at low field for **H**∥*c* are quantitative, because all parameters are determined only from the data of the FISC at high fields. In what follows, we explain the differences depending on the pairing symmetries.

The results for *s*-wave pairing are shown in Figs. 1 and 2. We obtain the effective-mass ratio $m_c/m_a=0.785$, which is reasonable in comparison with the value estimated from the Shubnikov–de Haas (SdH) oscillations.[41,42] It is confirmed that the FFLO state is not realized in the FISC. In contrast, it is shown that low-field superconductivity exhibits the FFLO state at low temperatures.
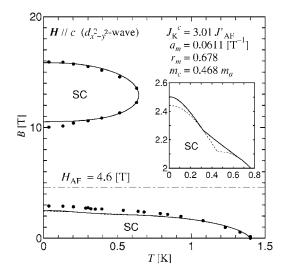

FIG. 3. Theoretical phase diagram for $d_{x^2-y^2}$-wave in the magnetic fields parallel to the *c* axis. The notation is the same as those in Fig. 1. The inset shows the theoretical phase diagram below 0.8 K and between 2 and 2.6 T.
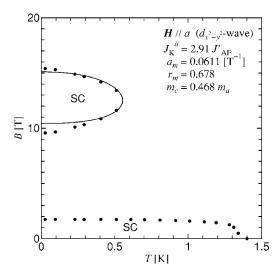
FIG. 4. Theoretical phase diagram for $d_{x^2-y^2}$-wave in the magnetic fields parallel to the a axis. The notation is the same as those in Fig. 1.

The results for $d_{x^2-y^2}$-wave pairing are shown in Figs. 3 and 4. We obtain $m_c/m_a=0.468$, which is too small in comparison with the value estimated from the SdH oscillations.[41,42] It is confirmed that the FFLO state is not realized in the FISC. There are bends in the theoretical curves of the low fields, where the Landau-level indexes n's of the optimum solution alternate. The solution near $T=0$ is expressed by a linear combination of the Abrikosov functions with odd n's. In Fig. 3, it is found that there are two tricritical points in the phase diagram for $\mathbf{H}\|c$. One at $T \simeq 0.67$ K is the critical point of the normal state, the BCS state with even n's, and the FFLO state with even n's, and another at $T \simeq 0.32$ K is that of the normal state, the FFLO states with even n's and odd n's.

The results for d_{xy}-wave pairing are shown in Figs. 5 and 6. We obtain $m_c/m_a=0.865$, which is reasonable in compari-
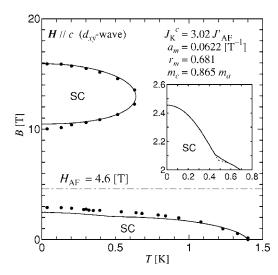

FIG. 5. Theoretical phase diagram for d_{xy}-wave in the magnetic fields parallel to the c axis. The notation is the same as those in Fig. 1. The inset shows the theoretical phase diagram below 0.8 K and between 2 and 2.6 T.
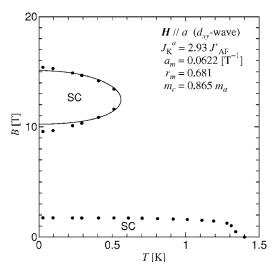

FIG. 6. Theoretical phase diagram for d_{xy}-wave in the magnetic fields parallel to the a axis. The notation is the same as those in Fig. 1.

son with the value estimated from the SdH oscillations.[41,42] In this case, the area of the FFLO state is very limited. It is found that the FFLO state is not realized in the FISC and low-field superconductivity near $T=0$. There is a bend in the
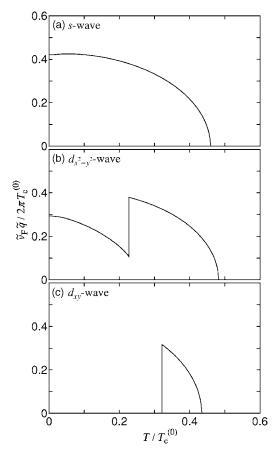

FIG. 7. Temperature dependence of the magnitudes of the total pair momentum along the upper critical field curves for (a) s-wave, (b) $d_{x^2-y^2}$-wave, and (c) d_{xy}-wave pairings in the magnetic fields parallel to the c axis. The sets of parameters for (a), (b), and (c) are the same as in Figs. 1, 3, and 5, respectively.

theoretical curve, where the parity of the Landau-level indexes n's alternates. The solution of the odd n's gives the highest critical field near $T=0$.

In Fig. 7, we show temperature dependences of $\tilde{q} \equiv (\tilde{m}/m_c)^{1/2}|\mathbf{q}|$ along the upper critical field curves of low-field superconductivity for s-wave, $d_{x^2-y^2}$-wave, and d_{xy}-wave pairings when $\mathbf{H}\|c$. For $d_{x^2-y^2}$-wave pairing, it is found that the $\tilde{q}$ jumps at a temperature where the Landau-level indexes n of the optimum solution alternate. For d_{xy}-wave pairing, it is found that the $\tilde{q}$ vanishes for $T < 0.32T_c^{(0)}$, where the FFLO state with odd n is unstable.

In a brief summary of this section, experimental results could be reproduced for all s-wave, $d_{x^2-y^2}$-wave, and d_{xy}-wave pairings. For s-wave pairing, the upper critical fields of low-field superconductivity are smaller than the experimental data, but they are improved by taking into account the FFLO state. The in-plane mass anisotropies are estimated as $m_c/m_a=0.785$, 0.468, and 0.865 for s-wave, $d_{x^2-y^2}$-wave, and d_{xy}-wave pairings, respectively. The results for s-wave and d_{xy}-wave pairings agree with the value obtained from the SdH oscillations,[41,42] whereas the result for $d_{x^2-y^2}$-wave pairing largely deviates from it. We found that the FFLO state does not occur in the FISC, while it occurs in low-field superconductivity.

V. SUMMARY AND DISCUSSION

We have studied the upper critical fields of antiferromagnetic s-wave, $d_{x^2-y^2}$-wave, and d_{xy}-wave superconductors with Fermi surface anisotropy. We have derived the linearized gap equations when the magnetic field is applied parallel to layers, taking into account the effective-mass anisotropy, the FFLO state, and the extended Jaccarino-Peter mechanism. We have applied the theory to the organic superconductor κ-(BETS)$_2$FeBr$_4$, and obtained good agreement between the theoretical and experimental results.

While the agreements have been obtained for all cases of s-wave, $d_{x^2-y^2}$-wave, and d_{xy}-wave pairings, the resultant in-plane mass ratios m_c/m_a are different from one another. The mass ratio for $d_{x^2-y^2}$-wave pairing seems too small, although those for s-wave and d_{xy}-wave pairings are close to the value estimated from the SdH oscillations.[41,42] The mass anisotropy dependence of the pure orbital limits of the upper critical fields is shown in Fig. 8. The upper critical fields for s-wave, $d_{x^2-y^2}$-wave, and d_{xy}-wave pairings become larger when the ratio m_c/m_a decreases. It is found that the upper critical field is the most influenced for d_{xy}-wave pairing by a change in the ratio m_c/m_a, while it is less influenced for $d_{x^2-y^2}$-wave pairing. This is why the resultant ratio m_c/m_a to fit the experimental data becomes much smaller for $d_{x^2-y^2}$-wave pairing than for d_{xy}-wave pairing.

This result is physically interpreted as follows. For example, we consider the situation that $m_c/m_a \lesssim 1$. The origin of the orbital pair-breaking effect is the Lorentz force that acts on electrons. When the magnetic fields are applied along the c axis, the Lorentz force is the strongest for electrons near the p_a axis, where the Fermi velocity is the largest, in the two-dimensional momentum space. When the mass ratio m_c/m_a decreases with the fixed electron number, i.e., when
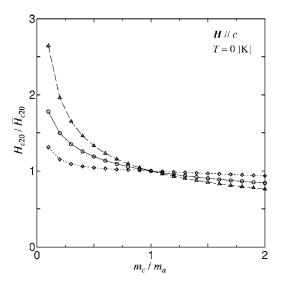

FIG. 8. The mass anisotropy dependence of the pure orbital limits for $\mathbf{H}\|c$. The open circles, open diamonds, and open triangles show the results for s-wave, $d_{x^2-y^2}$-wave, and d_{xy}-wave pairings, respectively. The solid, dotted, and dashed curves are guides to the eye. Here, $\bar{H}_{c20}$ denotes the orbital limit H_{c20} of the isotropic case ($m_c=m_a$).

the effective mass m_a increases, the Fermi velocity in the a direction decreases. Therefore, the Lorentz force acting on the electrons on the Fermi surface near the p_a axis becomes stronger and superconductivity is more suppressed when m_c/m_a decreases. The order parameter of $d_{x^2-y^2}$-wave pairing has nodes on the p_a axis, while that of d_{xy}-wave pairing has the largest amplitude there. Therefore, $d_{x^2-y^2}$-wave pairing is less affected than d_{xy}-wave pairing by a change in the ratio m_c/m_a.

It has been found from Fig. 5 that the FFLO state does not occur for d_{xy}-wave pairing in low-field superconductivity near $T=0$. This result is physically explained as follows. Since the effective density of states for α-wave pairing is proportional to $[\gamma_\alpha(\hat{\mathbf{p}})]^2$ in the gap equation, areas of the Fermi surface near the peak of $[\gamma_\alpha(\hat{\mathbf{p}})]^2$ have a greater effect on the nesting condition for the FFLO state, but those near the nodes of $[\gamma_\alpha(\hat{\mathbf{p}})]^2$ have less effect.[43] Hence, in the absence of the orbital pair-breaking effect, the vector $\mathbf{q}$ tends to points in the areas of the Fermi surfaces where $[\gamma_\alpha(\hat{\mathbf{p}})]^2$ exhibits a peak. In this study, however, we adopt the model in which $\mathbf{q}\|\mathbf{H}$ is assumed due to the orbital pair-breaking effect. Therefore, for d_{xy}-wave pairing, the Fermi surface nesting is less effective when $\mathbf{H}\|\hat{x}$ or $\hat{y}$, because the order parameter has nodes on the p_x and p_y axes. In contrast, for $d_{x^2-y^2}$-wave pairing, because the order parameter has peaks on the p_x and p_y axes, the FFLO state occurs in low-field superconductivity, when $\mathbf{H}\|\hat{x}$ or $\hat{y}$.

In the application to κ-(BETS)$_2$FeBr$_4$, it is found that the FFLO state is not present in the FISC in contrast to λ-(BETS)$_2$FeCl$_4$, while it is present in low-field superconductivity. In λ-(BETS)$_2$FeCl$_4$, the phase boundary of the FISC can be well reproduced if the possibility of the FFLO state is taken into account.[25] For the FFLO state to occur, the orbital pair-breaking effect needs to be sufficiently sup-

pressed. In λ-(BETS)$_2$FeCl$_4$, this condition seems to be satisfied even at high field due to low dimensionality. In contrast, it was suggested that κ-(BETS)$_2$FeBr$_4$ has a larger interlayer electron hopping energy than λ-(BETS)$_2$FeCl$_4$.[3] Therefore, in κ-(BETS)$_2$FeBr$_4$, the orbital effect is substantial at high fields, as verified by comparison of the zero-field transition temperature and the maximum transition temperature of the FISC.

The upper critical fields of low-field superconductivity agree with the experimental data, as shown in Figs. 1, 3, and 5. Further, for s-wave pairing, the agreement is improved if the FFLO state is taken into account. However, they are slightly smaller than the experimental data. This discrepancy may be removed by taking into account a mixing effect in the presence of the weak triplet pairing interaction, as in the compounds λ-(BETS)$_2$FeCl$_4$.[25] A slight discrepancy also occurs in the lower critical fields of the FISC, where the FFLO state does not occur as explained above. If the mixing effect occurs, this discrepancy may also be removed.

For $d_{x^2-y^2}$-wave and d_{xy}-wave pairings in low-field superconductivity, we found an internal transition between the vortex states with different Landau level indexes n, which is analogous to internal transitions in a two-dimensional system in tilted magnetic fields.[36] Both the FFLO state and the vortex state with higher n's originate from the Pauli paramagnetic effect as discussed in Ref. 36, because in the absence of Zeeman energy only the vortex state with lower n's occurs. Due to the transitions to the FFLO state and the vortex states with higher n's, the upper critical fields of low field superconductivity exhibit downward convex curves for all pairing symmetries examined, which agrees with the experimental data.

We have determined the microscopic parameters only from the curves of the FISC, and calculated the upper critical field of low-field superconductivity with those parameter values without any additional fitting parameters. From the accordance between the theoretical and experimental results on low-field superconductivity, the extended Jaccarino-Peter mechanism[7,8] seems to be realized in κ-(BETS)$_2$FeBr$_4$. Applying the extended Jaccarino-Peter mechanism to the same models with different parameter values, we obtain some unusual phase diagrams as shown in Fig. 9. When $J_K^c = 1.5 J'_{AF}$, the transition temperature curve has double peaks. When $J_K^c = J'_{AF}$, superconductivity occupies large area in the phase diagram. Similar phase diagrams have been obtained in two- and three-dimensional systems.[8,25] In this study, we confirmed that the phase diagrams as obtained above can be realized in a more realistic model of organic superconductors. If we control the value of J_K by material design, such critical field curves would be observed.

In the present theory, the effective mass m_b is included in the parameter a_m. Since we have obtained the value of a_m, we can estimate a value of m_b, if we have the value of $\tilde{p}_F$ appropriate for κ-(BETS)$_2$FeBr$_4$.
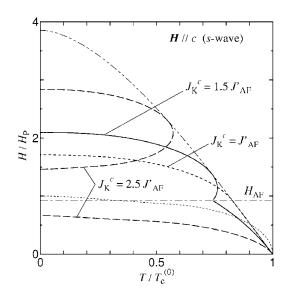

FIG. 9. Theoretical predictions of the phase boundary of superconductivity for various values of J_K^c. The other parameters are common to Fig. 1. The thin dotted and thin two-dot-dashed curves show the Pauli paramagnetic and orbital limits, respectively. In this figure, the FFLO state is taken into account, but modifies the curves slightly at low temperatures. At the upper critical fields of the FISC for $J_K^c = 2.5 J'_{AF}$, the FFLO state does not occur.

The upper critical field in low fields for $\mathbf{H}\|a$ could not be reproduced by the present theory. It has been found that the magnetic easy axis of antiferromagnetic long-range order in low fields is along the a axis,[10] and that the metamagnetic transition occurs at the antiferromagnetic phase boundary close to the upper critical field.[3] In order to reproduce the upper critical field in low fields for $\mathbf{H}\|a$, we need to reproduce the localized spin structure. This remains for future study.

In conclusion, the experimental phase diagrams of the antiferromagnetic superconductor κ-(BETS)$_2$FeBr$_4$ are theoretically reproduced by the present theory. In particular, the low-field phase for $\mathbf{H}\|c$ is well reproduced by the model parameters that are determined from the critical fields of the FISC. Therefore, the extended Jaccarino-Peter mechanism seems to be realized in the present compound at low fields. Due to this mechanism, some unusual phase diagrams may occur in compounds with appropriate energy parameters, in the future.

ACKNOWLEDGMENTS

[1] S. Uji, H. Shinagawa, T. Terashima, T. Yakabe, Y. Terai, M. Tokumoto, A. Kobayashi, H. Tanaka, and H. Kobayashi, Nature (London) **410**, 908 (2001).

[2] L. Balicas, J. S. Brooks, K. Storr, S. Uji, M. Tokumoto, H. Tanaka, H. Kobayashi, A. Kobayashi, V. Barzykin, and L. P. Gor'kov, Phys. Rev. Lett. **87**, 067002 (2001).

[3] T. Konoike, S. Uji, T. Terashima, M. Nishimura, S. Yasuzuka, K. Enomoto, H. Fujiwara, B. Zhang, and H. Kobayashi, Phys. Rev. B **70**, 094514 (2004).

[4] V. Jaccarino and M. Peter, Phys. Rev. Lett. **9**, 290 (1962).

[5] O. Cépas, R. H. McKenzie, and J. Merino, Phys. Rev. B **65**, 100502(R) (2002).

[6] Ø. Fisher, Helv. Phys. Acta **45**, 331 (1972).

[7] H. Shimahara, J. Phys. Soc. Jpn. **71**, 713 (2002).

[8] H. Shimahara, J. Phys. Soc. Jpn. **73**, 3121 (2004).

[9] B. S. Chandrasekhar, Appl. Phys. Lett. **1**, 7 (1962); A. M. Clogston, Phys. Rev. Lett. **9**, 266 (1962).

[10] H. Fujiwara, E. Fujiwara, Y. Nakazawa, B. Z. Narymbetov, K. Kato, H. Kobayashi, A. Kobayashi, M. Tokumoto, and P. Cassoux, J. Am. Chem. Soc. **123**, 306 (2001).

[11] V. L. Ginzburg, Zh. Eksp. Teor. Fiz. **23**, 236 (1952).

[12] N. R. Werthamer, in *Superconductivity*, edited by R. D. Parks (Marcel Dekker, New York, 1969), Vol. I, p. 321.

[13] P. C. Hohenberg and N. R. Werthamer, Phys. Rev. **153**, 493 (1967).

[14] C. T. Rieck and K. S. Scharnberg, Physica B **163**, 670 (1990).

[15] E. Langmann, Phys. Rev. B **46**, 9104 (1992).

[16] J.-H. Xu, Y. Ren, and C. S. Ting, Int. J. Mod. Phys. B **52**, 2699 (1996).

[17] W. Kim, J.-X. Zhu, and C. S. Ting, Phys. Rev. B **58**, R607 (1998); **61**, 4200 (2000).

[18] T. Kita and M. Arai, Phys. Rev. B **70**, 224522 (2004); M. Arai and T. Kita, J. Phys. Soc. Jpn. **73**, 2924 (2004).

[19] A. G. Lebed and K. Yamaji, Phys. Rev. Lett. **80**, 2697 (1998).

[20] A. G. Lebed and N. Hayashi, Physica C **341-348**, 1677 (2000).

[21] For a review, see R. Casalbuoni and G. Nardulli, Rev. Mod. Phys. **76**, 263 (2004).

[22] P. Fulde and R. A. Ferrell, Phys. Rev. **135**, A550 (1964); A. I. Larkin and Y. N. Ovchinnikov, Zh. Eksp. Teor. Fiz. **47**, 1136 (1964) [Sov. Phys. JETP **20**, 762 (1965)].

[23] L. W. Gruenberg and L. Gunther, Phys. Rev. Lett. **16**, 996 (1966).

[24] M. Houzet, A. Buzdin, L. Bulaevskii, and M. Maley, Phys. Rev. Lett. **88**, 227001 (2002); L. Bulaevskii, A. Buzdin, and M. Maley, *ibid.* **90**, 067003 (2003).

[25] H. Shimahara, J. Phys. Soc. Jpn. **71**, 1644 (2002); Physica B **329-333**, 1442 (2003).

[26] M. A. Tanatar, T. Ishiguro, H. Tanaka, and H. Kobayashi, Phys. Rev. B **66**, 134503 (2002).

[27] H. A. Radovan, N. A. Fortune, T. P. Murphy, S. T. Hannahs, E. C. Palm, S. W. Tozer, and D. Hall, Nature (London) **425**, 51 (2003).

[28] A. Bianchi, R. Movshovich, C. Capan, P. G. Pagliuso, and J. L. Sarrao, Phys. Rev. Lett. **91**, 187004 (2003).

[29] T. Watanabe, Y. Kasahara, K. Izawa, T. Sakakibara, Y. Matsuda, C. J. van der Beek, T. Hanaguri, H. Shishido, R. Settai, and Y. Onuki, Phys. Rev. B **70**, 020506(R) (2004).

[30] C. Martin, C. C. Agosta, S. W. Tozer, H. A. Radovan, E. C. Palm, T. P. Murphy, and J. L. Sarrao, Phys. Rev. B **71**, 020503(R) (2005).

[31] K. Kakuyanagi, M. Saitoh, K. Kumagai, S. Takashima, M. Nohara, H. Takagi, and Y. Matsuda, Phys. Rev. Lett. **94**, 047602 (2005).

[32] H. Adachi and R. Ikeda, Phys. Rev. B **68**, 184510 (2003).

[33] H. Won, K. Maki, S. Haas, N. Oeschler, F. Weickert, and P. Gegenwart, Phys. Rev. B **69**, 180504(R) (2004).

[34] K. Scharnberg and R. A. Klemm, Phys. Rev. B **22**, 5233 (1980).

[35] H. Shimahara, S. Matsuo, and K. Nagai, Phys. Rev. B **53**, 12 284 (1996).

[36] H. Shimahara and D. Rainer, J. Phys. Soc. Jpn. **66**, 3591 (1997).

[37] I. A. Luk'yanchuk and V. P. Mineev, Sov. Phys. JETP **66**, 1168 (1987).

[38] M. Prohammer and J. P. Carbotte, Phys. Rev. B **42**, 2032 (1990).

[39] R. A. Klemm and J. R. Clem, Phys. Rev. B **21**, 1868 (1980).

[40] M. Hamada and H. Shimahara, Phys. Rev. B **51**, 3027 (1995); J. Phys. Soc. Jpn. **65**, 552 (1996).

[41] T. Konoike, S. Uji, T. Terashima, M. Nishimura, S. Yasuzuka, K. Enomoto, H. Fujiwara, B. Zhang, E. Fujiwara, and H. Kobayashi, Phys. Rev. B **72**, 094517 (2005); T. Konoike, H. Fujiwara, B. Zhang, H. Kobayashi, M. Nishimura, S. Yasuzuka, K. Enomoto, and S. Uji, Physica C **412-414**, 107 (2004).

[42] L. Balicas, J. S. Brooks, K. Storr, D. Graf, S. Uji, H. Shinagawa, E. Ojima, H. Fujiwara, H. Kobayashi, A. Kobayashi, and M. Tokumoto, Solid State Commun. **116**, 557 (2000); S. Uji, H. Shinagawa, Y. Terai, T. Yakabe, T. Terashima, L. Balicas, J. S. Brooks, E. Ojima, H. Fujiwara, H. Kobayashi, A. Kobayashi, and M. Tokumoto, Physica B **298**, 557 (2001).

[43] H. Shimahara, J. Phys. Soc. Jpn. **66**, 541 (1997); **68**, 541 (1999); H. Shimahara and K. Moriwake, *ibid.* **71**, 1234 (2002).